

The effect of branching on slip and rheological properties of lubricants in molecular dynamics simulation of Couette shear flow

A. Jabbarzadeh^{*}, J.D. Atkinson, R.I. Tanner

School of Aerospace, Mechanical and Mechatronic Engineering, The University of Sydney, Sydney, NSW 2006, Australia

Received 5 April 2001; received in revised form 23 August 2001; accepted 30 August 2001

Abstract

Molecularly thin liquid films of alkane in extreme conditions in a thin film lubrication regime have been investigated. To get an insight into the effects of molecular architecture in the behaviour of these thin lubricant films we have studied six different molecules, mainly isomers of C_{30} . In this work the effect of branching on rheological properties and behaviour of lubricant film is examined. Our study shows viscosity and normal stress effects depend on the degree of branching. Dynamics of the molecules and their orientation are also affected by the degree of branching. A weaker layering near the wall is observed for branched molecules. Slip between the wall and lubricant film also was larger for branched molecules. Branched molecules had less tendency to change their orientation under the flow. The results obtained here could be helpful in designing new lubricants at the molecular level. © 2002 Published by Elsevier Science Ltd.

Keywords: Molecular dynamics computer simulation; Molecular structure; Boundary lubrication

1. Introduction

Experiments in modern tribology have shown that in boundary lubrication regime the thickness of the lubricating film reaches molecular dimensions and nanometer scales [1]. Experiments on these films have used novel microscopy techniques such as Surface Force Apparatus (SFA) and Atomic Force Microscopy (AFM). Although experiments have revealed many intriguing properties of ultrathin liquid films, it is still very difficult to determine all properties such as boundary conditions and fluid properties by experimental measurement. In these thin films the expected shear rates can be very high and beyond the values that can be studied by conventional means in laboratories. A 5-nm- (about 10 molecular diameter) thick lubricant film undergoing shear between two surfaces moving by 2.5 m/s velocity in opposite directions results in a very high shear rate of 10^9 s^{-1} . The shear thinning and normal stress effects observed at non-Newtonian regime then become of paramount importance in this situation. Molecular dynamics simulations, however, have proven an efficient method

in investigating these complex systems at high shear rates and extreme conditions. Several such studies have been conducted for simple liquids [2–4] and also for more complex linear chain molecules by various researchers [5–7]. These investigations have revealed the non-homogeneous nature of these thin films and strong layering near the walls. Shear thinning and normal stress effects are also observed in these simulations [5,7].

Growing demand for saving energy and reducing pollution levels have made the designing of new lubricants with better efficiency an important area of active research. A first step in designing better lubricants is to understand the structural effects of molecular architecture on the properties and performance of the lubricant film. The main objective of this study is to understand the effect of branching on the behaviour of lubricant films.

There have been many attempts to understand this problem both experimentally and computationally. Experiments by Muraki [8] in Elasto-Hydrodynamic Lubrication (EHL) conditions have revealed that shear stresses are larger for branched molecules and increase with degree of branching, resulting in a higher traction coefficient. In rolling element bearings lubrication studies, it has been shown that a higher degree of branching

^{*} Corresponding author.

has a negative effect on lubricant performance in certain applications [9]. Other experiments [10] with SFA for a branched molecule with a low degree of branching find lower friction coefficients in comparison to linear and shorter alkanes.

For much longer molecules of hyperbranched polymers [11] and low-density polyethylene (LDPE) [12], experiments have shown that viscosity, shear thinning and first normal stress difference are affected by the degree of branching.

Gao et al. [13] have done molecular dynamics simulations for simple branched molecules of squalane. They compared their results with those for hexadecane, revealing some dynamical and structural differences. They have shown diminished layering and in-plane order for squalane in comparison with linear molecules of hexadecane. Gupta et al. [7,14,22] have investigated squalane and linear alkanes, studying structural and rheological properties of thin films in general. However, no emphasis was put on the effect of branching.

In the present work we study thin confined lubricant films with the aim of obtaining insight into the effect of branching on various properties and behaviour of the lubricant. We mainly study different isomers of C₃₀ alkane to eliminate the effect of molecular weight. Five isomers with different degrees of branching are studied.

2. Simulation details

We have conducted molecular dynamics simulation for the study of thin liquid films confined between two solid atomic walls. Moving the walls in opposite directions to simulate the lubrication process generates Couette shear flow.

2.1. The walls

Each wall is comprised of three layers of atoms of a BCC (body centred cubic) lattice. Each atom on the wall is attached by a spring to its lattice position. The wall springs have a potential of the form

$$\phi_s = \frac{1}{2}k_w R^2 \quad (1)$$

where k_w is the spring stiffness and R is the distance of the wall atom from its lattice site. Here a soft spring with $k_w = 100\epsilon\sigma^{-2}$ is used, where σ and ϵ are the length and energy parameters for the CH₂ group given in Table 1. Periodic boundary conditions are applied in x and y directions only. As the results show, the amount of slip is large and, as in our early simulations for hexadecane [6], to reduce this a softer spring constant is used. In addition a structure-less wall inside the atomic wall which has a very short range is used to prevent the fluid molecules from penetrating the wall [6].

2.2. Model liquid

A United Atom model is used to model the alkane molecules. In this model, groups of CH, CH₂ and CH₃ are treated as single interaction sites. That is, carbon-hydrogen interactions are ignored by adjusting the mass and other parameters to compensate it. We will refer to these groups as atoms for simplicity. The Lennard–Jones (LJ) potential given by Eq. (2) (below) governs the interactions of the atoms belonging to different molecules and also those of the atoms on the same molecule separated by more than three atoms.

$$\phi_{LJ}(r) = 4\epsilon_{ij} \left[\left(\frac{\sigma_{ij}}{r} \right)^{12} - \left(\frac{\sigma_{ij}}{r} \right)^6 \right] - \phi_{\text{shift}}, \quad (2)$$

$$\phi_{\text{shift}} = 4\epsilon \left[\left(\frac{\sigma}{r_c} \right)^{12} - \left(\frac{\sigma}{r_c} \right)^6 \right]$$

The parameters used have produced results in good agreement with experiments for liquid–vapour coexistence curves for linear and branched alkanes [15,16]. In this model, the Lennard–Jones (LJ) energy parameter for methyl groups at the end of backbones is different from that for methyl groups at the end of branches. Also, different LJ parameters are used for a tertiary carbon CH group at the branch sites from those of a CH₂ group. The parameters for LJ interaction potentials are given in Table 1. For the interaction of unlike groups Lorentz–Berthelot’s combining rules are used so $\epsilon_{ij} = (\epsilon_i \epsilon_j)^{1/2}$ and $\sigma_{ij} = (\sigma_i + \sigma_j)/2$. For wall atoms the energy parameter is 16 times the energy parameter of CH₂ groups. This gives a value of 188 K for ϵ_w , the energy parameter for wall–CH₂ interactions. This is four times stronger than CH₂–CH₂ interactions and is close to a typical surface energy of metals. For a gold surface ϵ_w is about 220 K [23] and for other metal surfaces typical values in the same range can be used.

Intramolecular architecture including bond stretching, angle bending and torsional potentials are included in the model. These potentials are given respectively by the following equation.

$$\phi(r) = \frac{1}{2}k(r_{ij} - r_0)^2 \quad (3)$$

$$\phi(\theta) = \frac{1}{2}k_\theta(\cos \theta - \cos \theta_0)^2 \quad (4)$$

$$\phi(\alpha) = \sum_i^5 C_i (\cos \alpha)^i \quad (5)$$

The parameters for the intramolecular and intermolecular potentials are given in Table 1. The equilibrium bond angle at a branch site of CH is slightly smaller than that for other groups. Also for torsional potential for X–

Table 1
Parameters for the intramolecular and intermolecular interaction potentials

A) LJ potential	ϵ/k_B (K)	σ (nm)
CH ₃ , end group on the backbone	114	0.393
CH ₃ , side group	78	0.393
CH ₂ all methylene groups	47	0.393
CH groups	32	0.385
Wall atoms	752	0.393
<hr/>		
B) Bending angle potential $K_6=520$ kJ/mol, $\theta_0=114^\circ$	B) Bending angle potential at CH sites $K_6=520$ kJ/mol, $\theta_0=112^\circ$	
<hr/>		
C) Stretching potential $K=51\,600$ $\epsilon\sigma^{-2}$, $r_0=0.154$ nm		
<hr/>		
C) Torsional potential X–CH ₂ –CH ₂ –Y (kJ/mol) $C_0=9.2789$ $C_1=12.1557$ $C_2=13.1201$ $C_3=-3.0597$ $C_4=26.2403$ $C_5=-31.4950$	C) Torsional potential X–CH–CH ₂ –Y (kJ/mol) $C_0=3.4070$ $C_1=7.5003$ $C_2=1.6281$ $C_3=-15.3732$	
<hr/>		

CH₂–CH₂–Y (X and Y can be any group of atoms) interactions, the original Ryckaert–Bellemans [17] model is used since it is shown in Ref. 18 that the result does not change if the potential is replaced by values used in Siepmann et al.'s model in Refs. 15 and 16. For interactions that involve a branch site of tertiary carbon X–CH–CH₂–Y, different parameters are used as prescribed in Ref. 15.

To eliminate the effect of molecular weight we study five isomers of C₃₀ alkane with different degrees of branching. 3D snapshots, molecular structure and the chemical name of these molecules are shown in Table 2. To avoid their somewhat lengthy chemical names we will refer to these molecules with some generic names as indicated in Table 2. Degree of branching (*DB*) here is defined as the ratio of number of branches to the total number of carbon atoms along the backbone of the molecule. Tetracosane is simulated for comparison with squalane, which has an equal backbone length.

The simulations were conducted in isothermal conditions with fluid and wall temperatures kept at 480 K and 300 K, respectively. The thermal part of the velocities of wall and fluid particles are rescaled every few time steps in all three directions [5]. Details of this method, which is applied both to fluid atoms and wall atoms can be found in Ref. 19. To calculate the local properties such as the streaming velocity profiles and local density profiles we have used a slicing technique method, described in detail elsewhere [4,5]. For all the simulations here the average density of the lubricant film is 800 kg/m³. The thickness of lubricant is 7.2 nm. Other dimensions of the simulation box are given in Fig. 1.

Equations of motion were integrated by a leap-frog Verlet algorithm. Since branched molecules usually have longer relaxation times we used rather long simulations. The time step used in the simulation was 0.002 in reduced units. An equilibrium run of 100 000 time steps

was performed, followed by another 400 000 time steps to collect the results. At lower shear rates we ran the simulations for 1 000 000 time steps. We extended the simulation runs to 2 000 000 time steps for C₁₂(C₃)₆ with the highest degree of branching in this work. No noticeable changes were detected in the results.

Simulations were performed by a domain decomposition parallel algorithm [24] on a cluster of DEC Alpha 500/286 workstations using PVM (Parallel Virtual Machine) message passing software that provided good speedup and efficiency.

3. Rheological properties of the lubricant film

From an engineering point of view one of the important characteristics to be measured is the rheological properties of the lubricant film. For the simulations conducted here we computed many important properties of the film including viscosity, normal stress differences and normal pressure for various lubricants. We also investigated the effect of molecular structure on these properties.

3.1. Stress tensor



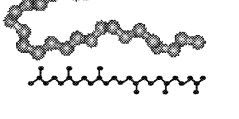
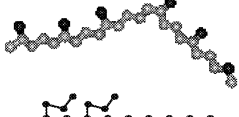

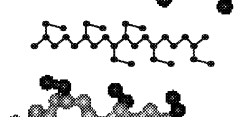
Stress tensor components were found for a microscopic system of particles by the Irving–Kirkwood [25] method. According to this method the contribution of each particle to the stress tensor is in two parts, a configuration part and a kinetic part. This can be written as

$$\sigma_{\alpha\beta} = -\frac{1}{V} \left\langle \sum_i m_i u_{i\alpha} u_{i\beta} + \sum_{i>j} \mathbf{r}_{ij\alpha} \mathbf{F}_{ij\beta} \right\rangle. \quad (6)$$

The first sum on the right-hand-side of Eq. (6) denotes

Table 2

Molecular structure, chemical name and degree of branching for the alkane molecules simulated here. Branches are shown with a darker shade to improve the clarity

Molecular Structure and a 3D snapshot	Chemical Name	Generic Name Used Here	DB
	C ₃₀ H ₆₂ (triacontane)	C ₃₀	0
	C ₂₄ H ₅₀ (tetracosane)	C ₂₄	0
	2,6,10,15,19,23, hexamethyltetracosane	Squalane	0.25
	2,6,13,17, tetrapropyloctadecane	C ₁₈ (C ₃) ₄	0.22
	2,6,9,10,13,17, hexaethyloctadecane	C ₁₈ (C ₂) ₆	0.33
	2,3,6,7,10,11, hexapropyldodecane	C ₁₂ (C ₃) ₆	0.5

the kinetic contribution where m_i is the atomic mass and α and β are coordination system axes, which for a Cartesian system can be simply substituted by X , Y or Z , and $u_{i\alpha}$ and $u_{i\beta}$ are the peculiar velocity components of particle i in the α and β directions. The second sum represents the configuration or potential contribution where $\mathbf{r}_{ij\alpha}$ is the α component of the distance vector between particles i and j and $\mathbf{F}_{ij\beta}$ is the β component of the force exerted on particle i by particle j . We have to exclude the mean flow velocity when we consider the laboratory velocity component of a particle in the flow direction. Then for shear stress we can rewrite Eq. (6) as

$$\sigma_{xz} = -\frac{1}{V} \left\langle \sum_i m_i u_{iz} [u_{ix} - U_{x,i}] + \sum_{i>j} \sum_{i,j} \mathbf{r}_{ijz} \mathbf{F}_{ijx} \right\rangle \quad (7)$$

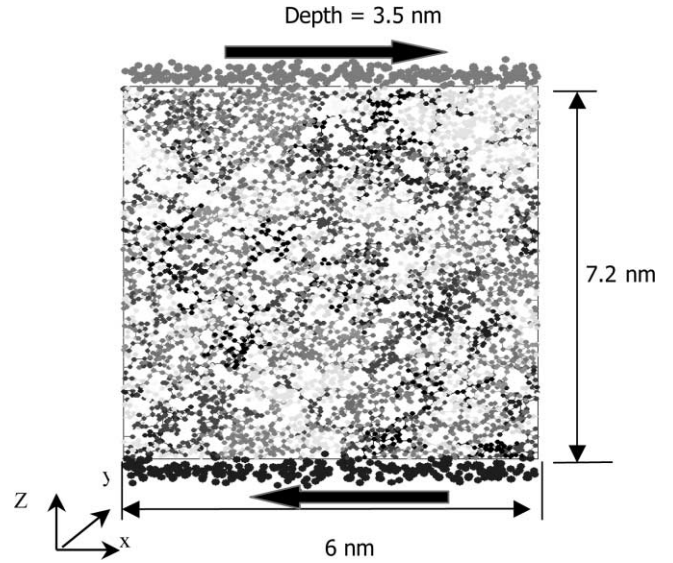


Fig. 1. Simulation box for Couette shear flow of C₁₂H₂₀(C₃H₇)₆ molecules. Molecules are shown with different shades to enhance the clarity of the snapshot.

where $U_{x,i}$ is the average flow velocity at the position of particle i . The angle brackets denote the time average.

Shear stress can also be computed from the time average of the force in the X direction applied to the wall particles by fluid particles during the simulation. Then we calculated the shear stress by dividing this force by the area of the walls. This shear stress is given by Eq. (8).

$$\sigma_{xz,w} = \sum_i \sum_j^{N_w, N_F} \mathbf{F}_{x,ij} / A. \quad (8)$$

In Eq. (8) $\mathbf{F}_{x,ij}$ represents forces in the x direction on a wall particle from the fluid particles. In the results presented here Eq. (8) is used for the calculation of shear stress (σ_{xz}). For other components of stress tensor Eq. (6) was used.

3.2. Viscosity and material functions

The average film viscosity is calculated from the following definition

$$\eta = \frac{\sigma_{xz}}{\dot{\gamma}} \quad (9)$$

The first and second normal stress differences are defined as

$$\begin{aligned} N_1 &= \sigma_{xx} - \sigma_{zz} \\ N_2 &= \sigma_{zz} - \sigma_{yy} \end{aligned} \quad (10)$$

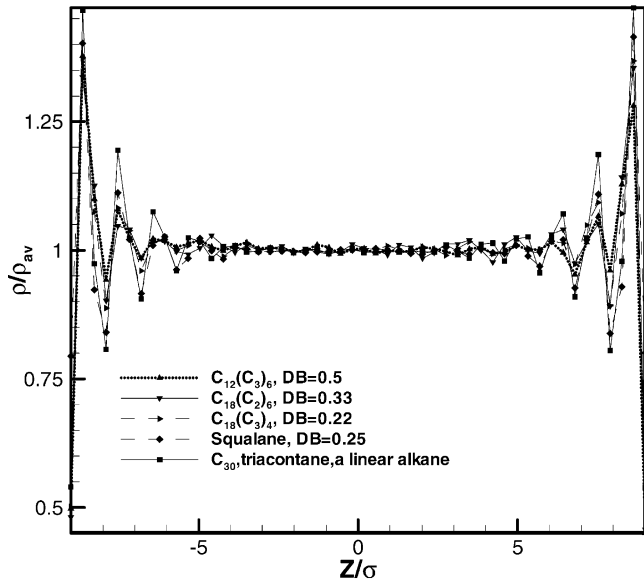


Fig. 2. Density profiles for different isomers of $C_{30}H_{62}$ with different degrees of branching.

4. Results

4.1. The effect of branching on density profiles

We calculated the density profiles for five isomers of the C_{30} molecule (Fig. 2). The applied shear rates for all the cases was 10^{10} s^{-1} . The figure shows the inhomogeneous density distributions, which indicate the layering of lubricant molecules near the wall. Moving toward the center of the film the density oscillations vanish to an almost constant density about the average film density. This is a well-known phenomenon for highly confined films of liquids. A closer look at the profiles near the walls in Fig. 3 shows that the layering of the lubri-

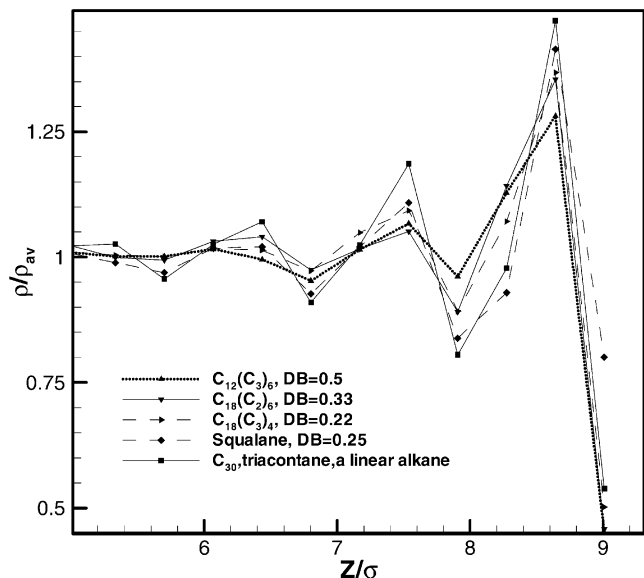


Fig. 3. Same density profiles shown in Fig. 2 close to the wall.

cant molecules is affected by the degree of branching. The strongest layering for linear C_{30} molecules occurs at the highest maxima and lowest minima in the density oscillation near the wall. Oscillations are weakest for the $C_{12}(C_3)_6$ molecule with the highest degree of branching. The number of layers for linear C_{30} and isomers with lower degrees of branching is three near each wall. For $C_{12}(C_3)_6$ there seems to be only two well-formed layers near each wall. Wang et al. [20] obtained similar results for linear *n*-octane and branched iso-octane. In a similar geometry to Wang et al.'s work, Gao et al. [13] reported similar observations in their grand canonical molecular dynamics simulations for hexadecane and squalane. Although no flow was involved in their simulations stronger layering was observed for hexadecane compared with branched molecules of squalane. We can conclude from these results that as the degree of branching increases the layering effect near the walls becomes weaker and the number of layers also decreases. This is an important factor in many applications where the formation of a film near the solid boundaries in molecular dimensions is important.

4.2. Slip

We calculated the velocity profiles for the lubricant film under Couette shear flow. The results show there is significant slippage between the solid boundary and the liquid film. Velocity profiles are shown for a typical shear rate of 10^{10} s^{-1} for all the isomers of C_{30} molecule and also tetracosane in Fig. 4. The slip on the wall greatly depends on the molecular degree of branching with

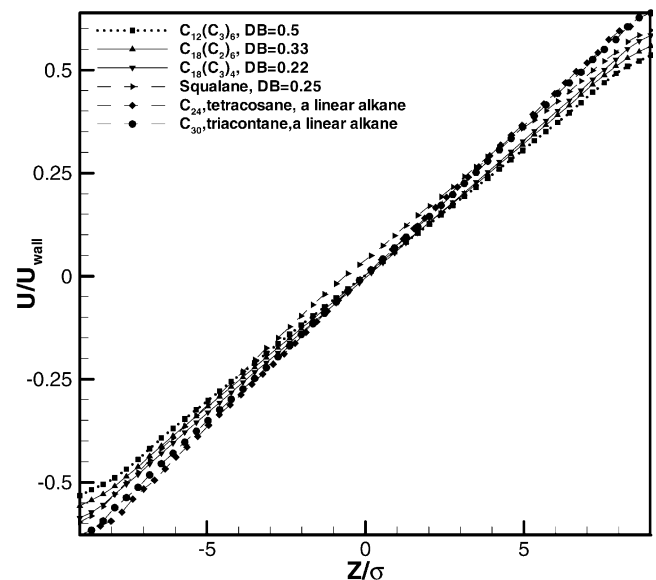


Fig. 4. Velocity profiles for various molecules with different degrees of branching. For all simulations the applied shear rate was 10^{10} s^{-1} . The y axis shows the ratio of streaming velocity to wall velocity. Values of 1 at the top wall and -1 at the lower wall mean a non-slip boundary condition.

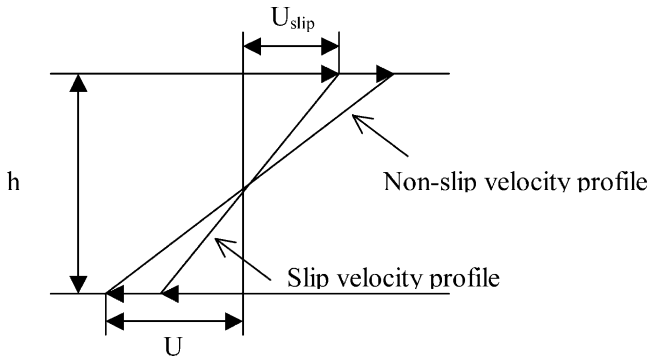


Fig. 5. This diagram shows how the velocity profiles are used to calculate the slip. Note that the shear rates are defined as $\dot{\gamma} = \frac{2U}{h}$ and $\dot{\gamma}_{\text{eff}} = \frac{2U_{\text{slip}}}{h}$. Slip is defined by Eq. (11).

the highest slip observed for $C_{12}(C_3)_6$ and the lowest for linear C_{30} and C_{24} . This means the effective shear rate experienced by the fluid film is smaller than the applied shear rate. The effective shear rate can be measured by fitting a line to the velocity profiles.

We quantified the slippage by defining the slip as:

$$\text{Slip} = 1 - \frac{\dot{\gamma}_{\text{eff}}}{\dot{\gamma}} \quad (11)$$

where $\dot{\gamma}_{\text{eff}} = \frac{\partial U}{\partial Z}$ is the effective shear rate, which is calculated by fitting the velocity data to a straight line. This is further explained in Fig. 5. So Slip=0 and Slip=1 respectively represent non-slip and complete slip conditions. We have plotted slip against the shear rate where applied shear ranges from 10^9 – $10^{11.5} \text{ s}^{-1}$. The results are shown in Fig. 6.

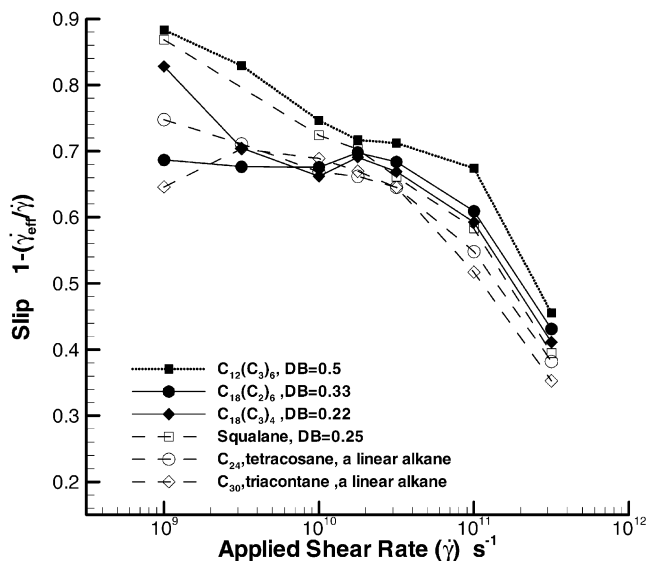


Fig. 6. Slip against the applied shear rate for various isomers of C_{30} and also linear tetracosane molecules.

The results show that the slip for all the molecules decreases as the applied shear rate is increased. This is the sort of results that we have obtained in our earlier work with hexadecane films [6,5] for surfaces with lower interaction energy. Gupta et al. [7] also reported a decrease in slip with increase in the applied shear rate in their simulations for hexadecane and squalane. Although the wall–fluid energy parameter used here is larger than that is used in hexadecane simulations we still see results of surfaces with low adsorption energy. This, however, can be explained by the higher molecular weight for the lubricants used here. Also in the refined potential model that is used here, end methyl groups have higher energy parameter values than those used in our earlier simulations, and these end groups can have some effects on the results. However, we speculate that this is mostly molecular weight related. In previous studies [4,6,21] we have shown that there are many parameters that affect the boundary conditions and the slip in these highly confined films. Parameters such as the wall–fluid interaction energy, film thickness, shear rate together with geometrical properties such as the wall roughness and the size of fluid constituent particles can all affect the slip. Here we are emphasising the effect of molecular structure on the boundary conditions. We can clearly see from Fig. 6 the slip is larger for branched molecules and in fact it increases as the degree of branching increases.

This clearly has implications in choosing the right liquid for desired applications. For example, for a traction fluid which we expect to have the highest possible traction coefficient and torque transmission, a branched molecule is probably not a suitable choice.

4.3. Rheological properties

4.3.1. Viscosity

Apparent shear viscosity of the lubricant film is calculated from Eq. (9). As we observed in Section 4.2 there is some slip between the film and solid wall so that the actual shear rate experienced by the lubricant film is smaller than the applied shear rate. The effective shear rate, however, is calculated as described in Section 4.2. The effective shear viscosity (η_{eff}) is calculated from the shear stress and the effective shear rate using Eq. (9). We have calculated both viscosities for shear rate ranging from 10^9 s^{-1} to $10^{11.5} \text{ s}^{-1}$. The result for the apparent shear viscosity as a function of the applied shear rate is given in Fig. 7 on a logarithmic scale. From this figure we can see that the apparent viscosity is larger for branched molecules and as the degree of branching increases viscosity increases. A shear thinning effect also appears on the results. However, the onset of shear thinning is not very clear. It seems that for branched molecules it starts at lower shear rates than for linear molecules of tetracosane and triacontane. We have fitted the

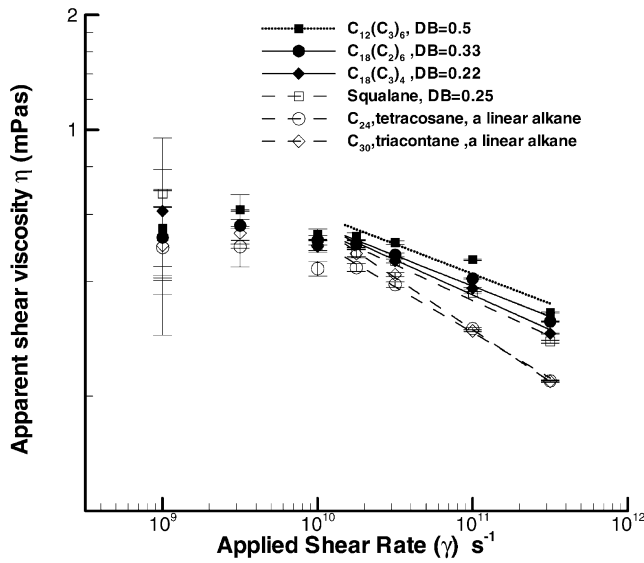


Fig. 7. Apparent shear viscosity of for molecules with various degrees of branching. Lines are power fit to viscosity data.

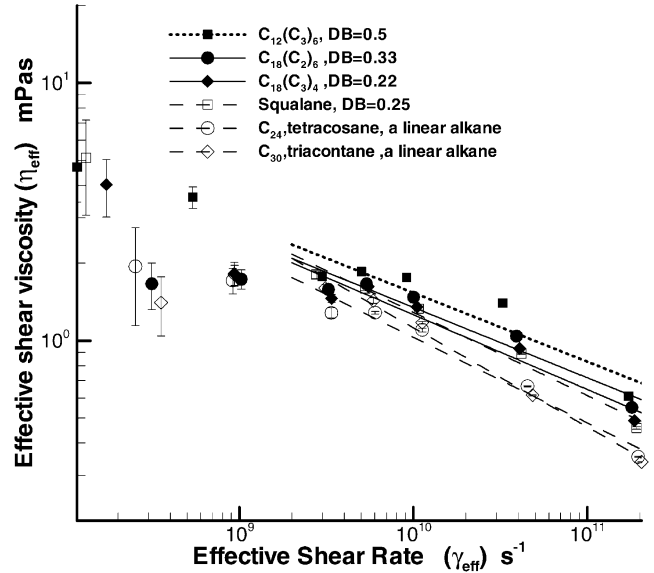


Fig. 8. Effective viscosity against the effective shear rate.

viscosity data to power fit lines for the region where the shear rate is higher than 10^{10} s^{-1} where shear thinning happens. It seems the viscosity obeys a power law with shear rate $\eta \propto \dot{\gamma}^{-\alpha}$. The value of the exponent, however, seems to be dependent on the type of molecule. The exponent α is given for these molecules in Table 3. It can be seen from this table that the exponent value decreases as the degree of branching increases. This means for apparent shear viscosity the shear thinning effect is weaker for branched molecules and gets weaker as the degree of branching increases. Linear alkanes exhibit stronger shear thinning in these simulations.

The results for the effective shear viscosity of the lubricant film are plotted in Fig. 8. The effective shear rate is dependent on the slip, which is different for each molecule type. So the viscosity points are not exactly at the same shear rates for all molecules. Here the effective shear rate is in the range 10^8 – 10^{11} s^{-1} . We can see from the results that here also the effective viscosity is larger for branched molecules and increases with the degree of branching. Shear thinning is also observed and effective viscosity obeys a power law with the shear rate in the form of $\eta_{\text{eff}} \propto \dot{\gamma}_{\text{eff}}^{-\alpha}$. The onset of shear thinning seems to happen at lower shear rates for some branched molecules; however, because of the large uncertainty at lower shear rates we cannot be certain of this. In experi-

ments with low-density polyethylene (LDPE) by Wood-Adams [12] increased viscosity and increased susceptibility to shear thinning was similarly observed as the degree of branching was increased. It should be noted that in this work a technique was employed to synthesise samples with almost the same molecular weight with different degrees of branching. We have fitted the data to power fit lines where shear thinning starts for all molecules. The exponent value is listed in Table 4 for different molecules with their degree of branching. Here we can see the exponent values are larger than those obtained for apparent viscosity. So the shear thinning is in fact stronger than that which might be measured from observation. We still see that the exponent is generally larger for linear molecules. It is somewhat dependent on the degree of branching and decreases with it. The only exception is squalane, which has a higher *DB* (0.25) than $C_{18}(C_3)_4$ ($DB=0.22$). However, it could be due to their close *DB* values, which also give an equal exponent value for apparent viscosity. This is discussed further in Section 5.

The exponent value for squalane is much lower than that reported by Gupta et al. [14] which is close to 0.6 for slightly higher density (820 kg/m^3) but lower fluid temperature of 300 K. The film thickness (9.25σ) used by them also is about half that in this work (18.356σ).

Table 3

The exponent value for power law behaviour of apparent viscosity for different molecules. Note that all the molecules except tetracosane (C_{24}) have the same molecular weight)

Molecule	$C_{12}(C_3)_6$	$C_{18}(C_2)_6$	$C_{18}(C_3)_4$	Squalane	C_{24}	C_{30}
α	0.15	0.16	0.18	0.18	0.23	0.27
<i>DB</i>	0.5	0.33	0.22	0.25	0	0

Table 4

The exponent value for power law behaviour of effective viscosity for different molecules

Molecule	C ₁₂ (C ₃) ₆	C ₁₈ (C ₂) ₆	C ₁₈ (C ₃) ₄	Squalane	C ₂₄	C ₃₀
α	0.26	0.27	0.29	0.32	0.33	0.39
DB	0.5	0.33	0.22	0.25	0	0

The viscosity for squalane at a temperature of 484 K and an effective shear rate of 0.032 in reduced units is reported to be 1.97 mPaS. Interpolating our results we find a lower viscosity of 1.17 mPaS at that shear rate. It seems the higher exponent and viscosity reported by the above authors stem from the higher density and thinner films used in their experiments, since both are known to increase the viscosity [5] and exponent [14]. This exponent does not seem to have a universal value and depends on many factors such as density, wall–fluid interaction strength and film thickness. Here we are more interested in the effect of molecular structure and qualitatively we can say that the branched molecules exhibit higher shear viscosity, but with weaker shear thinning effect. Sendjarevic and McHugh [11] have performed experiments with high molecular weight hyperbranched polymers of polyesters and poly(ether-imide) with various degrees of branching. Interestingly, their findings are in agreement with our findings, showing shear thinning effect becomes weaker as the degree of branching is increased. Despite the much lower shear rates (1–100 s⁻¹) used in the mentioned experiments [11,12] with long polymers their results correspond well with ours. In fact the relaxation time for the long, high molecular weight, and hyperbranched molecules that they have tested is many orders higher than the short molecules that we have examined here. So the high shear rates we have used here are offset by their long relaxation times.

4.3.2. Normal stress differences

We have also calculated normal stress differences for various shear rates and the results are plotted against applied shear rate in Fig. 9. The first normal stress has a positive value for all cases. The results show generally higher values of N_1 for branched molecules. The same conclusion is made in Wood-Adams' [12] experiments with LDPE, where a higher first normal stress coefficient was found by increasing the degree of branching. In the non-linear regime at higher shear rates there is significant enhancement of N_1 with increasing shear rate.

In this region N_1 follows a power-law behaviour with shear rate in the form of $N_1 \propto \dot{\gamma}^\alpha$ as shown with power-fit lines. The exponent, however, seems to be smaller for branched molecules as can be seen from the data listed in Table 5. Except for squalane it seems the exponent value increases and the degree of branching decreases. Plotting N_1 against the effective shear rate also gives the same picture, except with slightly lower values for α .

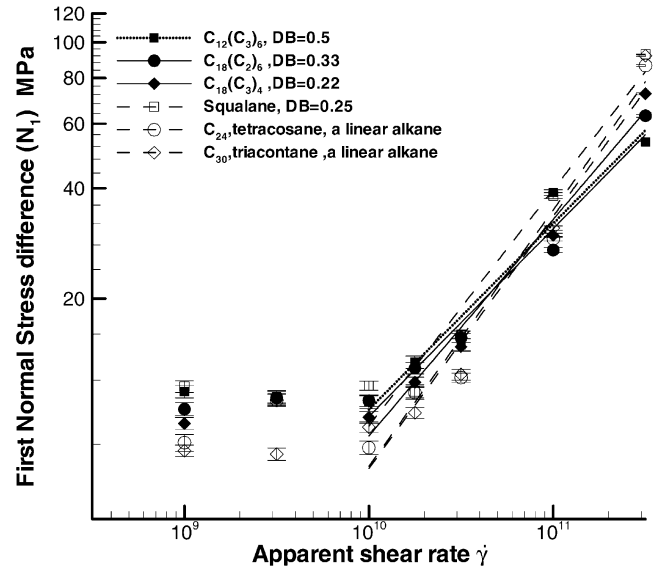


Fig. 9. First normal stress difference versus apparent shear rate in logarithmic scale.

Here also we get a good agreement with the experiments conducted by Sendjarevic and McHugh [11] for hyperbranched polymers of polyesters and poly(ether-imide). They observed the normal stress effect gets weaker with increasing degree of branching by obtaining lower exponent values for polymers with higher degree of branching.

We also calculated the second normal stress difference N_2 that was negative for all cases. The absolute ratio of $|N_1/N_2|$ is plotted against the effective shear rate in Fig. 10. At lower shear rates this ratio is close to unity as both have almost the same magnitude. As the shear rate is increased, in about the same region as the non-linear effects are observed, the increase in this ratio means that N_1 grows faster than N_2 , and it seems that the rate of growth is higher for linear molecules than for branched ones.

4.4. Molecular orientation

4.4.1. Orientation with the wall

We have studied the dynamics and molecular orientation of these molecules. Time average for the square of direction cosine ($\cos^2\theta$) of the bonds on the backbone with respect to the Z axis (normal to the walls) are calculated for each molecule. This orientation factor is a measure of how the molecules are oriented with respect to

Table 5

The exponent in power law behaviour of N_1 with respect to applied shear rates and also the effective shear rate for various molecules

Molecule	$C_{12}(C_3)_6$	$C_{18}(C_2)_6$	$C_{18}(C_3)_4$	Squalane	C_{24}	C_{30}
$\alpha (N_1 \text{ vs. } \dot{\gamma})$	0.51	0.51	0.59	0.65	0.69	0.7
$\alpha (N_1 \text{ vs. } \dot{\gamma}_{\text{eff}})$	0.42	0.44	0.51	0.60	0.59	0.64
DB	0.5	0.33	0.22	0.25	0	0

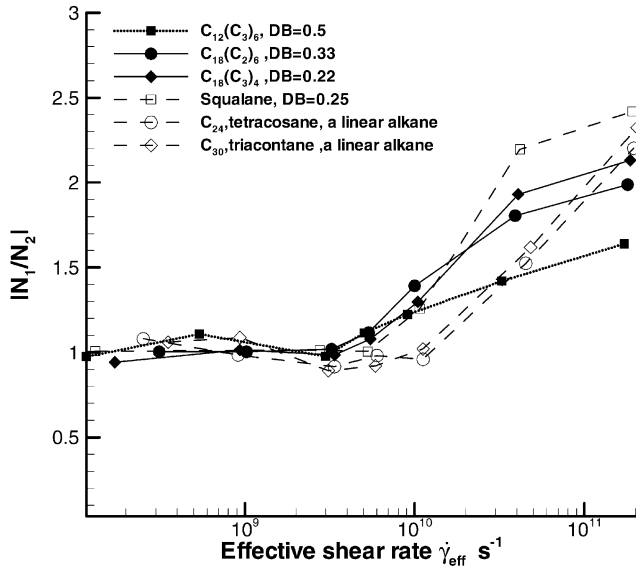


Fig. 10. Ratio of first and second normal stress differences against the applied shear rate.

the wall. Its range is 0–1 and a value closer to zero indicates a more parallel orientation with the wall. This orientation factor is shown in Fig. 11 against the applied shear rate. We observe in this figure that for the branched

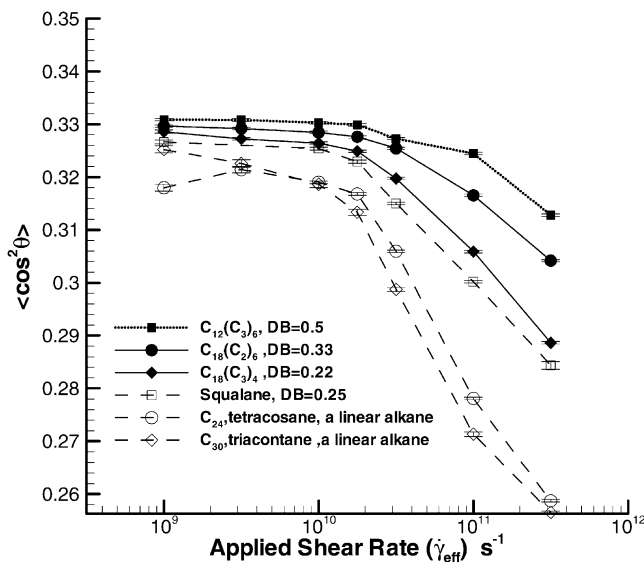


Fig. 11. Orientation factor with respect to the wall for various molecules. Values closer to zero indicate a more parallel orientation toward the walls.

molecules the orientation factor has a higher value for all the cases.

This means branched molecules have less tendency than their linear counterparts to align parallel to the wall. In fact we can see as the degree of branching increases the orientation factor also increases. Squalane, however, which should have a higher value than $C_{18}(C_3)_4$, exhibits a lower value. We will discuss this discrepancy later. As the shear rate increases we can see that for all the molecules studied here the tendency to align parallel to the wall increases. However, the shear-induced alignment is much stronger for linear alkanes. As the degree of branching increases shear-induced alignment decreases.

4.4.2. Molecular conformation

Time average end to end distances as a function of the effective shear rate for all the molecules are shown in Fig. 12. We can see that it hardly changes with shear rate for $C_{12}(C_3)_6$. For $C_{18}(C_3)_4$ and $C_{18}(C_2)_6$ also the change is very small but noticeable. For squalane and two linear alkanes we can see that the change in end to end distance under shear is more significant. There is an indication that the linear alkanes and also squalane to a lesser degree become fully stretched under shear. It can be seen that molecular conformations of the branched

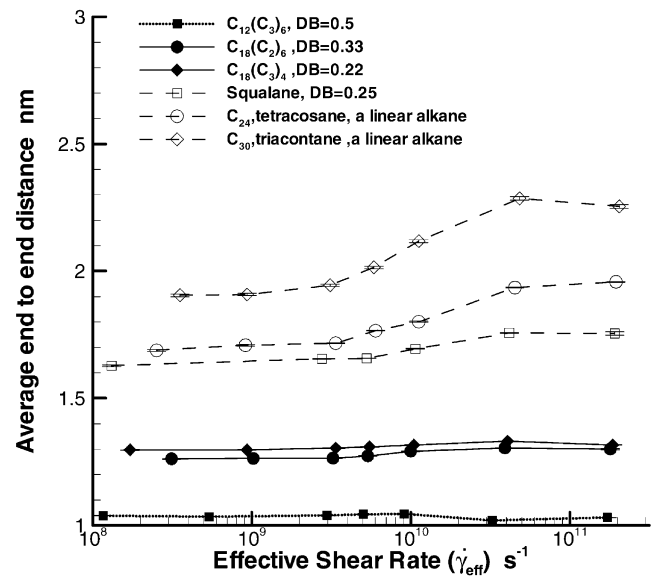


Fig. 12. Average end to end distance of the molecules for different molecules shows the conformation of the branched molecules is less affected by the flow.

alkanes do not change under shear. This can also be confirmed from the snapshots that we have taken from the top side of the simulation box as shown for various molecules in Fig. 13. The snapshots are taken at a shear rate of $3.16 \times 10^{11} \text{ s}^{-1}$ for all cases. Only molecules within a layer of about 1.5σ next to the wall are shown in these snapshots. These are the molecules in the first layer next to the wall. We can see that for $C_{12}(C_3)_6$ there is not a preferred orientation and most of the molecules are distributed randomly. For $C_{18}(C_2)_6$ no preferential orientation can be observed. For $C_{18}(C_3)_4$, which has a lower degree of branching, it seems that to some degree there is a preferred orientation of the backbone in the direction of the flow. For squalane and linear triacontane and tetracosane this orientation in flow direction is quite obvious. Comparing C_{24} and squalane we can see that for tetracosane the chain conformation is usually fully stretched in the flow direction. For squalane there is a tendency for folding that is not seen for C_{24} . We have confirmed this folding tendency for squalane by producing animations of the molecular movements. In simulations by Gao et al. [13] for squalane and hexadecane similar observations were reported with higher in-plane ordering for hexadecane molecules. We have shown here that this ordering is reduced by branching.

5. Discussion and conclusions

Molecular dynamics simulations were conducted for highly confined films of lubricants in high shear rates and pressures in boundary lubrication regime. The objective was to get an insight into fundamental properties and behaviour of the lubricant and the effect of molecular structure on those properties. We put our emphasis on the effect of branching on the various properties of lubricant film. We defined degree of branching as the ratio of the number of branches to the number of carbon atoms on the backbone (backbone length) and measured the properties of many isomers of C_{30} alkane with various degrees of branching. The results showed there was a systematic correlation between the degree of branching and many important properties of the film. In the results, despite the higher *DB* value for squalane, it came after $C_{18}(C_3)_4$ when categorised based on the degree of branching. This was almost the same story for slip, orientation factor, end to end distance, viscosity and normal stresses. We speculate that length of molecules and the fact that squalane length is closer to the linear alkanes have something to do with this out-of-the-ordinary behaviour. To investigate this further we divided *DB* by the backbone length of each molecule and the

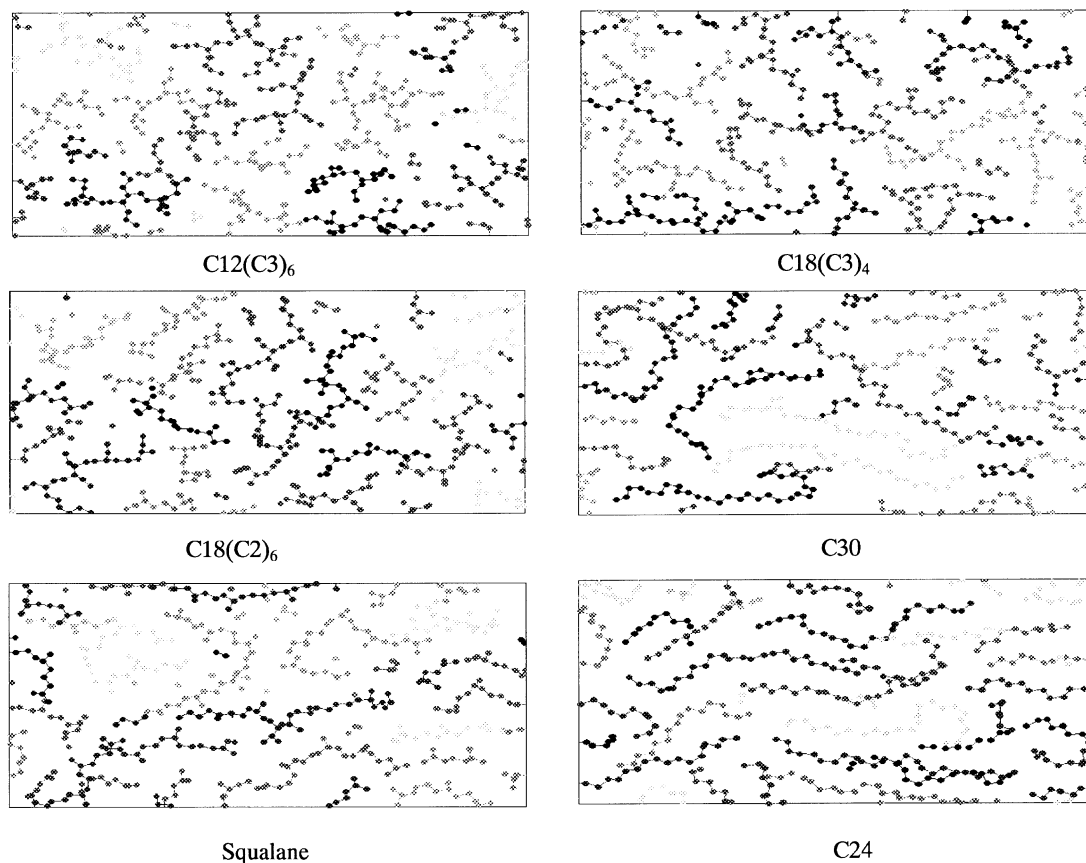


Fig. 13. Snapshots from the top view (*xy* plane) for different molecules. All the snapshots are taken at applied shear rates of $10^{11.5} \text{ s}^{-1}$. Flow induced conformation changes are less than that for linear alkanes.

Table 6

Reduced degree of branching DB^* for various molecules. Here b , n and m are the number of branches, backbone length and branch length, respectively

Molecule ($C_n(C_m)_b$)	$C_{12}(C_3)_6$	$C_{18}(C_2)_6$	$C_{18}(C_3)_4$	Squalane	C_{24}	C_{30}
Backbone length (n)	12	18	18	24	24	30
$DB=b/n$	0.5	0.33	0.22	0.25	0	0
$DB^*=b/n^2$	0.0417	0.0183	0.0122	0.0104	0	0

values obtained for a reduced degree of branching DB^* are given in Table 6. We can see that according to these values squalane comes after $C_{18}(C_3)_4$ and has a smaller reduced degree of branching. So we think the reduced degree of branching can be a more useful parameter to account for the effect of branching with respect to its relative length. So in these concluding remarks when we refer to degree of branching we mean DB^* unless stated otherwise.

We found that branched molecules had weaker layering and also the number of layers formed near the wall could be affected by the degree of branching. It is interesting that experiments in the EHL regime by Jonsson [9] show that lubricants with a higher degree of branching have lower film forming capability. We also found that slip boundary conditions prevailed for all the lubricants examined here. The slip was larger for branched lubricants and increased with the degree of branching. We also found higher viscosities for branched molecules. The viscosity increased with degree of branching in agreement with the experiments [8] in EHL conditions and contrary to experiments with SFA [10]. In SFA experiments mentioned here, however, the only branch molecule used was 2-methyloctadecane, which has a very low degree of branching ($DB=0.06$). Also the film thickness was in the order of only 3–5 molecular diameter which was much thinner than our film thickness (18σ). We plan to conduct further studies on much thinner films to clarify this.

The shear thinning effect was observed and we found that this effect got stronger as the degree of branching decreased. This is an important finding, showing that branched alkanes might have a better performance in extreme high shear rates where the thinning effect of the viscosity can have harmful consequences to machinery. First normal stress difference calculations showed higher values for branched alkanes. Dependence of the normal stress effect to shear rate was stronger for linear alkanes and as the degree of branching increased the rate of increase in N_1 decreased. Our findings for the effect of the degree of branching on shear thinning and normal stress effects were in agreement with the experiment for much longer hyperbranched polymer solutions [11]. In these simulations, however, molecular weight of the samples was not in the same range. More recent experi-

ments by Wood-Adams [12] on low density polyethylene has used a technique to vary the long chain branching (LCB) independently from the molecular weight. The results of these experiments are also in good agreement with our results. Wood-Adams has found viscosity and first normal stress difference enhancement by increasing LCB. Also increased susceptibility to shear thinning was observed for higher LCB polymers where the onset of shear thinning happened at lower shear rates. We could also observe this from our viscosity data.

The conformation and orientation of branched molecules were less affected by the wall and also the flow. We found that as the degree of branching is increased the ordering effect under the flow is decreased. The tendency of linear alkanes to orient in the flow direction can be one of the reasons why they exhibit higher shear thinning and normal stress effects at higher shear rates as they stretch in the flow direction.

Acknowledgements

We gratefully acknowledge support for this study by an Australian Research Council (ARC) grant. We wish also to thank the Sydney Distributed Computing (SyDCom) Laboratory for the generous time allocated to us on the computing facility.

References

- [1] Dowson D. Thin films in tribology. In: Proceedings of the 19th Leeds–Lyon Symposium on Tribology, 1992:3–12.
- [2] Thompson PA, Robbins MO. Shear flow near solids: Epitaxial order and flow boundary conditions. *Phys Rev A* 1990;41:6830–7.
- [3] Thompson A, Grest GS, Robbins MO. *Phys Rev Lett* 1992;68:3448–51.
- [4] Jabbarzadeh A, Atkinson JD, Tanner RI. Rheological properties of thin liquid films by molecular dynamics simulations. *J Non-New Fluid Mech* 1997;69:169–93.
- [5] Jabbarzadeh A, Atkinson JD, Tanner RI. Nanorheology of molecularly thin films of n-hexadecane in couette shear flow by molecular dynamics simulation. *J Non-New Fluid Mech* 1998;77:53–78.
- [6] Jabbarzadeh A, Atkinson JD, Tanner RI. Wall slip in the molecular dynamics simulation of thin films of hexadecane. *J Chem Phys* 1999;110:2612–20.

- [7] Gupta SD, Cochran HD, Cummings PT. Shear behavior of squalane and tetracosane under extreme confinement. Model, simulation method, and interfacial slip. *J Chem Phys* 1997;107:10316–26.
- [8] Muraki M. Molecular structure of synthetic hydrocarbon oils and their rheological properties governing traction characteristics. *Tribol Int* 1987;20:347–54.
- [9] Jonsson UJ. Lubrication of rolling element bearings with HFC-polyolester mixtures. *Wear* 1999;232:185–91.
- [10] Gee ML, McGuiggan PM, Israelachvili JN. Liquid to solid like transitions of molecularly thin films under shear. *J Chem Phys* 1990;93:1895–906.
- [11] Sendjarevic I, McHugh AJ. Effects of molecular variables and architecture on the rheological behaviour of dendritic polymers. *Macromolecules* 2000;33:590–6.
- [12] Wood-Adams P. The effect of long chain branches on the shear flow behaviour of polyethylene. *J Rheol* 2001;45:203–10.
- [13] Gao J, Luedtke WD, Landman U. Structure and solvation forces in confined films: Linear and branched alkanes. *J Chem Phys* 1997;106:4309–17.
- [14] Gupta SD, Cochran HD, Cummings PT. Shear behavior of squalane and tetracosane under extreme confinement. III. Effect of confinement on viscosity. *J Chem Phys* 1997;107:10335–43.
- [15] Siepman JI, Martin MC, Mundyand CJ, Klien ML. Intermolecular potentials for branched alkanes and the vapour liquid phase equilibria of n-heptane, 2-methylhexane, and 3-ethylpentane. *Mol Phys* 1997;90:687–93.
- [16] Cui ST, Cummings PT, Cochran HD. Configurational bias Gibbs ensemble Monte Carlo simulation of vapor–liquid equilibration of short and branched alkanes. *Fluid Phase Equil* 1997;141:45–61.
- [17] Ryckaert JP, Bellemans A. Molecular dynamics of liquid n-butane near its boiling point. *Chem Phys Lett* 1975;30:123–5.
- [18] Smit B, Karaborni S, Siepman I. Computer simulations of vapor–liquid phase equilibria of n-alkanes. *J Chem Phys* 1994;102:2126–40.
- [19] Brown D, Clarke HR. *Mol Phys* 1984;51:1243–52.
- [20] Wang Y, Hill K, Harris JG. Confined thin films of a linear and branched octane. A comparison of the structure and solvation forces using molecular dynamics simulations. *J Chem Phys* 1993;100:3276–85.
- [21] Jabbarzadeh A, Atkinson JD, Tanner RI. The effect of the wall roughness on slip and rheological properties of hexadecane in molecular dynamics simulation of Couette shear flow between two sinusoidal walls. *Phys Rev E* 2000;61:690–9.
- [22] Gupta SD, Cochran HD, Cummings PT. Shear behavior of squalane and tetracosane under extreme confinement. II. Confined film structure. *J Chem Phys* 1997;107:10327–34.
- [23] Xia TK, Ouyang J, Ribarsky MW, Landman U. Interfacial alkane films. *Phys Rev Lett* 1992;69:1967–70.
- [24] Jabbarzadeh A, Atkinson JD, Tanner RI. Parallel simulation of shear flow of polymers between structured walls by molecular dynamics simulation on PVM. *Comput Phys Commun* 1997;107:123–36.
- [25] Irving JH, Kirkwood JG. The statistical mechanical theory of transport process. IV. The equations of hydrodynamics. *J Chem Phys* 1950;18:817–29.